Wilfried Elmenreich, J. Tenreiro Machado and Imre J. Rudas (Eds)

Intelligent Systems

at the Service of Mankind

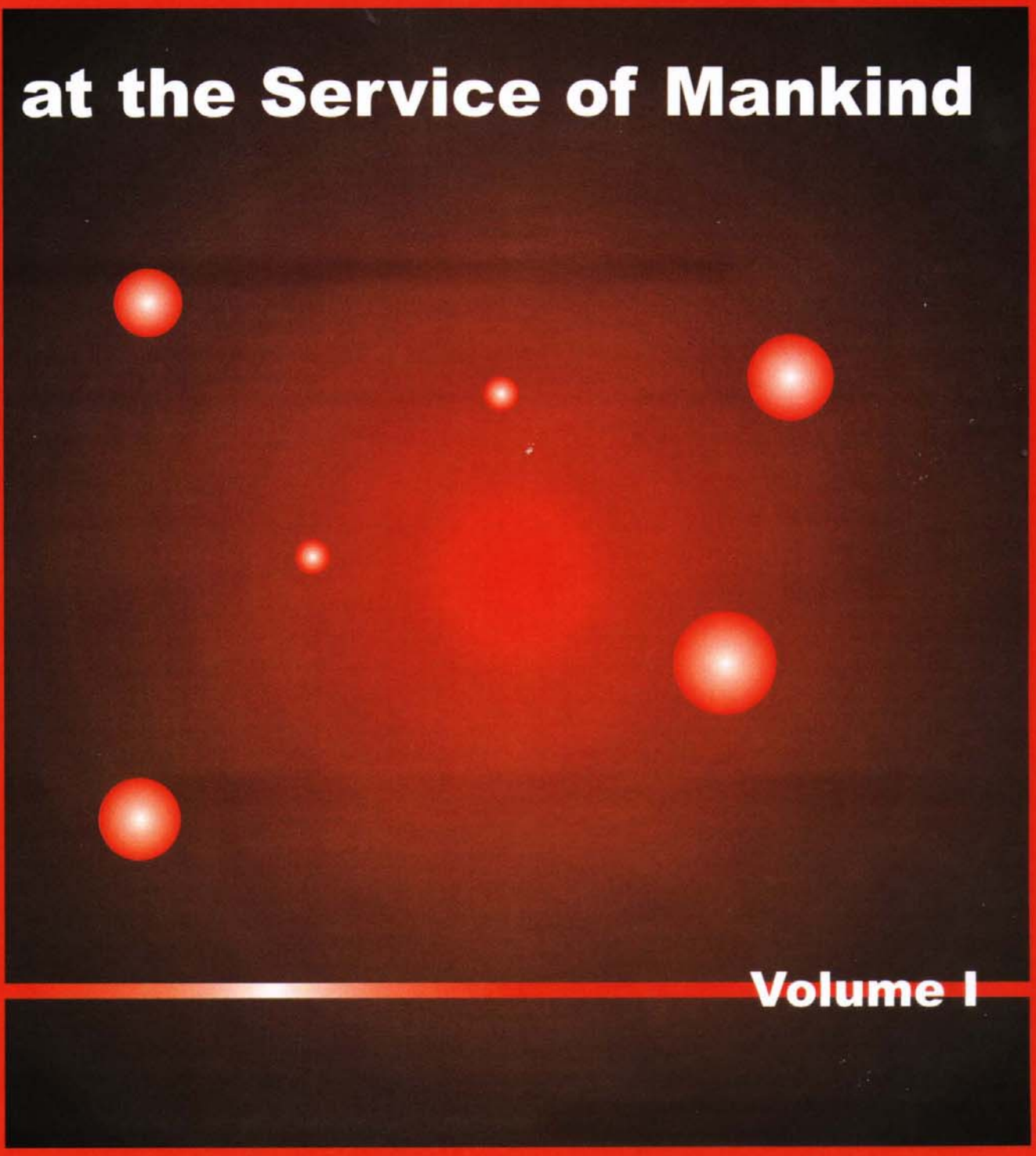

Volume I

Analysis of Systems with Backlash and Impacts through the Describing Function

Ramiro S. Barbosa and J. A. Tenreiro Machado

Institute of Engineering,
Polytechnic Institute of Porto, Porto, Portugal
{rbarbosa,jtm}@dee.isep.ipp.pt

***Abstract* —** *This paper analyses the dynamical properties of systems with backlash and impact phenomena based on the describing function method. The dynamics is illustrated using the Nyquist and Bode plots and the results are compared with those of standard models.*

1 Introduction

The area of Fractional Calculus (FC) deals with the operators of integration and differentiation to an arbitrary (including noninteger) order and is as old as the theory of classical differential calculus. The theory of FC is a well-adapted tool to the modelling of many physical phenomena, allowing the description to take into account some peculiarities that classical integer-order models simply neglect. For this reason, the first studies and applications involving FC had been developed in the domain of fundamental sciences, namely in physics [5] and chemistry [23]. Besides the intensive research carried out in the area of pure and applied mathematics [1–5], FC has found applications in various fields such as viscoelasticity/damping [6–12], chaos/fractals [13–16], biology [17], signal processing [18], system identification [19], diffusion and wave propagation [20–21], electromagnetism [22] and automatic control [24–29]. Nevertheless, in spite of the work that has been done in the area, the application of these concepts has been scarce until recently. In the last years, the advances in the theory of fractals and chaos revealed subtle relationships with FC, motivating a renewed interest in this field.

The phenomenon of vibration with impacts occurs in many branches of technology where it plays a very useful role. On the other hand, its occurrence is often undesirable, because it causes additional dynamic loads, as well as faulty operation of machines and devices. Despite many investigations that have been carried out so far, this phenomenon is not yet fully understood, mainly due to the considerable randomness and diversity of reasons underlying the energy dissipation involving the dynamic effects [32–38].

In this paper we investigate the dynamics of systems that contain backlash and impacts.

Bearing these ideas in mind, the article is organized as follows. Section 2 introduces the fundamental aspects of the describing function method. Section 3 studies the describing function of systems with backlash and impact phenomena. Finally, section 4 draws the main conclusions and addresses perspectives towards future developments.

2 Describing Function Analysis

The describing function (DF) is one of the possible methods that can be adopted for the analysis of nonlinear systems [31]. The basic idea is to apply a sinusoidal signal in the input of the nonlinear element and to consider only the fundamental component of the signal appearing at the output of the nonlinear system. Then, the ratio of the corresponding phasors (output/input) of the two sinusoidal signals represents the DF of the nonlinear element. The use of this concept allows the adaptation of the Nyquist stability test to a nonlinear system detection of a limit cycle, namely the prediction of its approximate amplitude and frequency. In this line of thought, we consider the control-loop with one nonlinear element N and a linear system $G(s)$ depicted in Fig. 1.

We start by applying a sinusoid $x(t) = X \sin(\omega t)$ to the nonlinearity input. At steady-state the output of the nonlinear characteristic, $y(t)$, is periodic and, in general, it is nonsinusoidal. If we assume that the nonlinearity is symmetric with respect to the variation around zero, the Fourier series becomes:

$$y(t) = \sum_{k=1}^{\infty} Y_k \cos(k\omega t + \phi_k) \tag{1}$$

where Y_k and ϕ_k are the amplidude and the phase shift of the k^{th}-harmonic component of the output $y(t)$, respectively.

In the DF analysis, we assume that only the fundamental harmonic component of $y(t)$, Y_1, is significant. Such assumption is often valid since the higher-harmonics in $y(t)$, Y_k for $k = 2, 3, \ldots$, are usually of smaller amplitude than the amplitude of the fundamental component Y_1. Moreover, most systems are "low-pass filters" with the result that the higher-harmonics are further attenuated. Thus the DF of a nonlinear element, $N(X,\omega)$, is defined as the complex ratio of the fundamental harmonic component of output $y(t)$ with the input $x(t)$:

$$N(X,\omega) = \frac{Y_1}{X} e^{j\phi_1} \tag{2}$$

where X is the amplitude of the input sinusoid $x(t)$ and Y_1 and ϕ_1 are the amplitude and the phase shift of the fundamental harmonic component of the output $y(t)$, respectively. In general, $N(X,\omega)$ is a function of both the amplitude X and the frequency ω of the input sinusoid. For nonlinear systems that do not involve energy storage, the DF is merely amplitude-dependent, that is $N = N(X)$. If it is not the case, we may have to adopt a numerical approach because, usually, it is impossible to find a closed-form solution.

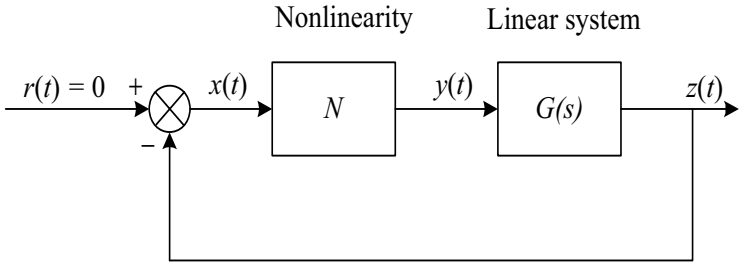

Figure 1: Basic nonlinear feedback system for describing function analysis

For the nonlinear control system of Figure 1, we have a limit cycle if the sinusoid at the nonlinearity input regenerates itself in the loop, that is:

$$G(j\omega) = -\frac{1}{N(X,\omega)} \tag{3}$$

Note that (3) can be viewed as the characteristic equation of the nonlinear feedback system of Figure 1. If (3) can be satisfied for some value of X and ω, a limit cycle is *predicted* for the nonlinear system. Moreover, since (3) applies only if the nonlinear system is in a steady-state limit cycle, the DF analysis predicts only the presence or the absence of a limit cycle and cannot be applied to analysis for other types of time responses.

3 Analysis of Systems with Backlash and Impacts

In this section, we use the DF method to analyse systems with backlash and impacts. We start by considering the standard static model and afterwards we study the case with the impact phenomena. Finally, we compare the results of the two types of approximations.

3.1 Static Backlash

Here we consider the phenomena of clearance without the effect of the impacts, which is usually called *static backlash*. The describing function for $X > h/2$ is given by [30]:

$$N(X) = \frac{k}{2}\left[1 - N_s\left(\frac{X/h}{1-X/h}\right)\right] - j\frac{2kh(X-h/2)}{\pi X^2} \tag{4a}$$

$$N_s(z) = \frac{2}{\pi}\left[\sin^{-1}\frac{1}{z} + \frac{1}{z}\cos\left(\sin^{-1}\frac{1}{z}\right)\right] \tag{4b}$$

The classical backlash model corresponds to the DF of a linear system of a single mass M_1+M_2 followed by the geometric backlash having as input and as output the position variables $x(t)$ and $y(t)$, respectively, as depicted in Figure 2. For a sinusoidal input force $f(t) = F\cos(\omega t)$ the condition $X = h/2$ leads to the limit frequency ω_L applicable to this system:

$$\omega_L = \left[\frac{2}{h}\frac{F}{(M_1+M_2)}\right]^{\frac{1}{2}} \tag{5}$$

Figure 3 shows the Nyquist plot of $-1/\mathrm{N}(F,\omega) = -1/[G(j\omega)N(X)]$ for several values of the input force F.

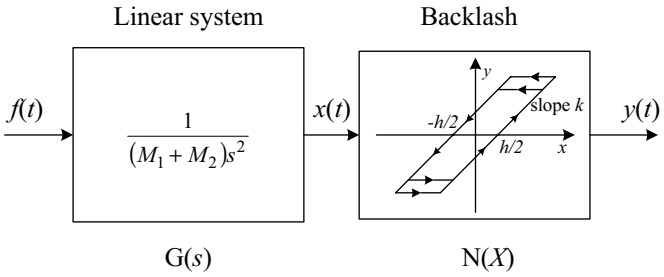

Figure 2: Classical backlash model

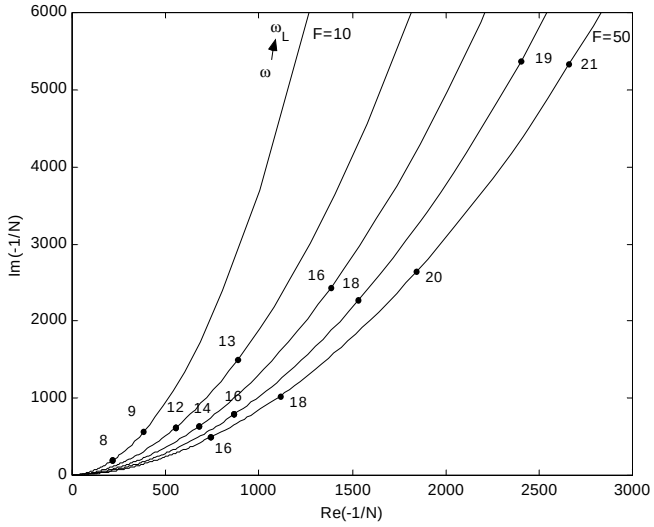

Figure 3: Nyquist plot of $-1/\mathrm{N}(F,\omega)$ for the system of Figure 2, $F = \{10, 20, 30, 40, 50\}$ N, $0 < \omega < \omega_L$, $M_1 = M_2 = 1$ kg and $h = 10^{-1}$ m

This approach to the backlash study is based on the adoption of a geometric model that neglects the dynamic phenomena involved during the impact process. Due to this reason often real results differ significantly from those predicted by that model.

3.1 Dynamic Backlash

In this section we use the DF method to analyse systems with backlash and impact phenomena, usually called *dynamic backlash* [33–34].

The proposed mechanical model consists on two masses (M_1 and M_2) subjected to backlash and impact phenomenon as shown in Figure 4. A collision between the masses M_1 and M_2 occurs when $x_1 = x_2$ or $x_2 = h+x_1$. In this case, we can compute the velocities of masses M_1 and M_2 after the impact ($\dot{x}_1'$ and $\dot{x}_2'$) by relating them to the previous values ($\dot{x}_1$ and $\dot{x}_2$) through Newton's rule:

$$\left(\dot{x}_1' - \dot{x}_2'\right) = -\varepsilon\left(\dot{x}_1 - \dot{x}_2\right), \quad 0 \le \varepsilon \le 1 \tag{6}$$

where ε is the coefficient of restitution. In the case of a fully plastic (*inelastic*) collision ε = 0, while in the *ideal elastic* case ε = 1.

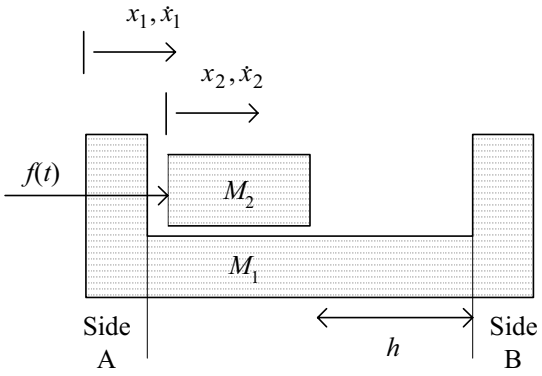

Figure 4: System with two masses subjected to dynamic backlash

By application of the principle of conservation of momentum $M_1\dot{x}_1' + M_2\dot{x}_2' = M_1\dot{x}_1 + M_2\dot{x}_2$ and of expression (6) we can find the sought velocities ($\dot{x}_1'$ and $\dot{x}_2'$) of both masses after an impact, given by:

$$\dot{x}_1' = \frac{\dot{x}_1(M_1 - \varepsilon M_2) + \dot{x}_2(1+\varepsilon)M_2}{M_1 + M_2},\ \dot{x}_2' = \frac{\dot{x}_1(1+\varepsilon)M_1 + \dot{x}_2(M_2 - \varepsilon M_1)}{M_1 + M_2} \tag{7}$$

For the system of Figure 4 we calculate numerically the Nyquist diagram of $-1/\mathrm{N}(F,\omega)$ for an input force $f(t) = F\cos(\omega t)$ applied to mass M_2 and considering the output position $x_1(t)$ of mass M_1.

The values of the parameters adopted in the subsequent simulations are $M_1 = M_2 = 1$ kg and $h = 10^{-1}$ m. Figures 5 and 6 show the Nyquist plots for $F = 50$ N and $\varepsilon = \{0.1, 0.2, 0.3, 0.4, 0.5, 0.6, 0.7, 0.8, 0.9\}$ and for $F = \{10, 20, 30, 40, 50\}$ N and $\varepsilon = \{0.2, 0.5, 0.8\}$.

The Nyquist charts of Figures 5–6 reveal the occurrence of a jumping phenomenon, which is a characteristic of nonlinear systems. This phenomenon is more visible around $\varepsilon \approx 0.5$, while for the limiting cases ($\varepsilon \to 0$ and $\varepsilon \to 1$) the singularity disappears. Moreover, shows also that for a fixed value of ε the charts are proportional to the input amplitude F.

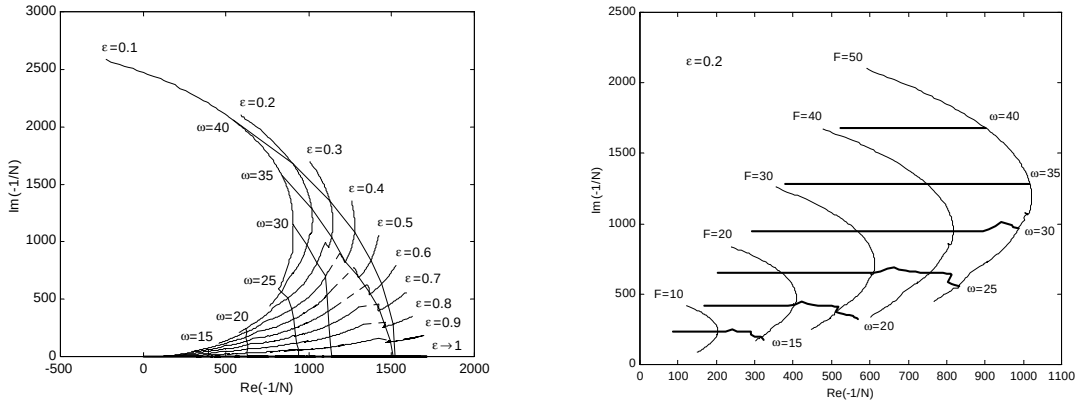

Figure 5: Nyquist plot of $-1/\mathrm{N}(F,\omega)$ for a system with dynamic backlash, for $F = 50$ N and $\varepsilon = \{0.1, .., 0.9\}$ and $F = \{10, 20, 30, 40, 50\}$ N and $\varepsilon = 0.2$

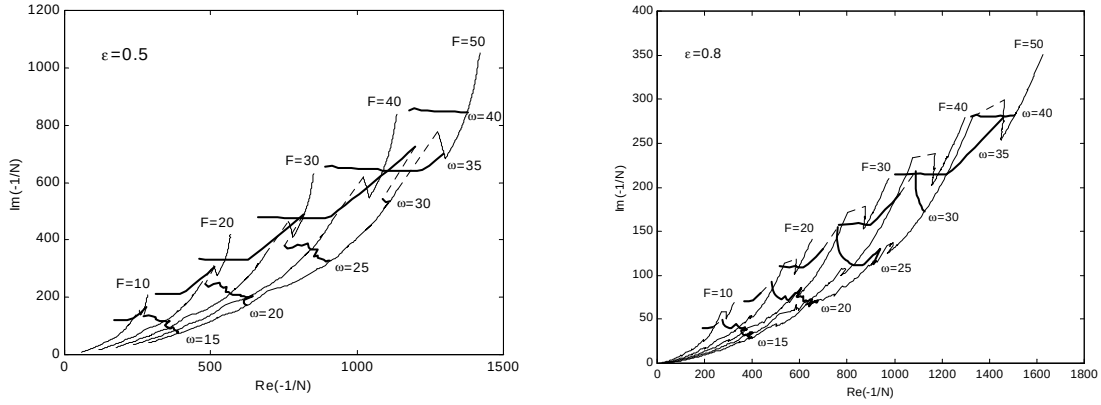

Figure 6: Nyquist plot of $-1/\mathrm{N}(F,\omega)$ for a system with dynamic backlash, for $F = \{10, 20, 30, 40, 50\}$ N and $\varepsilon = \{0.5, 0.8\}$

The validity of the proposed model is restricted to frequencies of the exciting input force $f(t)$ higher than a lower-limit frequency ω_C. On the other hand, there is also an upper-limit frequency ω_L determined by application of Newton's law to mass M_2 and considering that the amplitude of the displacement is within the clearance $h/2$. In the middle-range frequency, $\omega_C < \omega < \omega_L$, the jumping phenomena occurs at frequency ω_J. These frequencies are given by the following expressions:

$$\omega_c \approx \left[\left(2\frac{F}{M_2 \cdot h}\right)^2 \cdot (1-\varepsilon)^5\right]^{\frac{1}{4}},\ \omega_L = 2 \cdot \left(\frac{F}{h \cdot M_2}\right)^{\frac{1}{2}},\ \omega_J \sim \left(\frac{F}{h \cdot M_2}\right)^{\frac{1}{2}} \tag{8}$$

Figures 7 and 8 illustrate the variation of the Nyquist plots of $-1/N(F,\omega)$ for the cases of the static and dynamic backlash and shows the log-log plots of $\mathrm{Re}\{-1/N\}$ and $\mathrm{Im}\{-1/N\}$ *versus* ω for a coefficient of restitution $\varepsilon = 0.5$ and $F = \{10, 20, 30, 40, 50\}$ N and for an input force $F = 50$ N and $\varepsilon = \{0.1, 0.3, 0.5, 0.7, 0.9\}$, respectively.

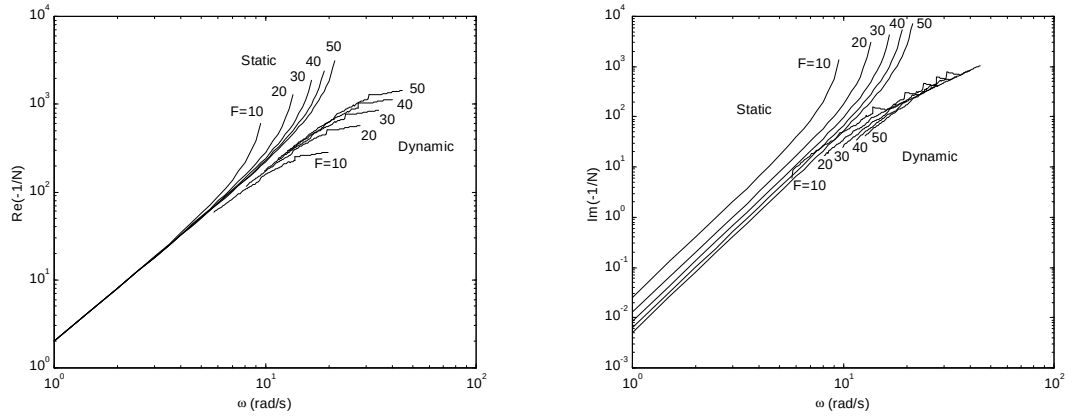

Figure 7: Log-log plots of $\mathrm{Re}\{-1/N\}$ and $\mathrm{Im}\{-1/N\}$ *versus* the exciting frequency ω, for $\varepsilon = 0.5$ and $F = \{10, 20, 30, 40, 50\}$ N

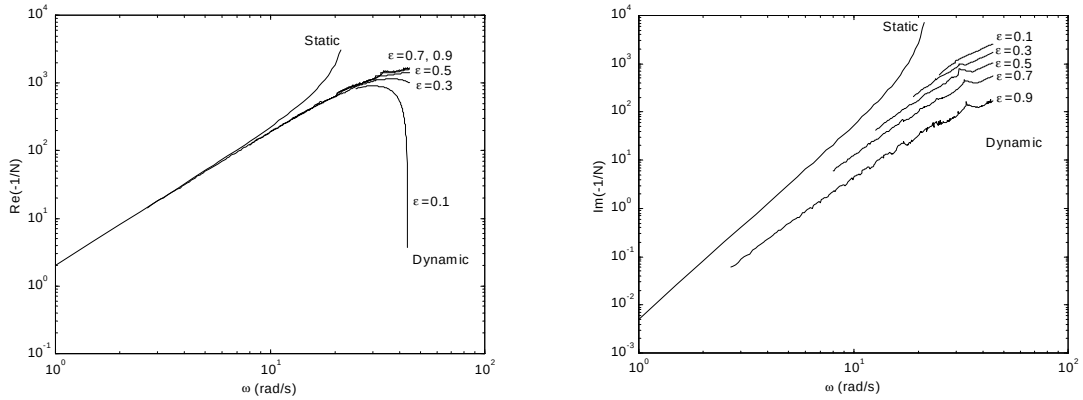

Figure 8: Log-log plots of $\mathrm{Re}\{-1/N\}$ and $\mathrm{Im}\{-1/N\}$ *versus* the exciting frequency ω, for $F = 50$ N and $\varepsilon = \{0.1, 0.3, 0.5, 0.7, 0.9\}$

Comparing the results for the static and the dynamic backlash models we conclude that:

- The charts of Re{−1/N} are similar for low frequencies (where they reveal a slope of +40 dB/dec) but differ significantly for high frequencies.
- The charts of Im{−1/N} are different in all range of frequencies. Moreover, for low frequencies, the dynamic backlash has a fractional slope inferior to +80 dB/dec of the static model.

A careful analysis must be taken because it was not demonstrated that a DF fractional slope would imply a fractional-order model. In fact, in this study we adopt integer-order models for the system description but the fractional-order slope is due to continuous/discrete dynamic variation that results due to the mass collisions.

Figure 9 presents the Fourier transform of the output displacement of mass M_1, $F\{x_1(t)\}$, namely the amplitude of the harmonic content of $x_1(t)$ for an input force $f(t) = 50\cos(\omega t)$, $\omega_C < \omega < \omega_L$, and $\varepsilon = \{0.2, 0.8\}$. The charts reveal that the fundamental harmonic of the output has a much higher magnitude than the other higher-harmonic components. This fact enables the application of the describing function in the prediction of limit cycles for this system. Nevertheless, for high values of ε, there is a significant high-order harmonic content, and by consequence, a lower precision of the limit cycle prediction.

Figures 10–14 show the time response of the output velocity $\dot{x}_1(t)$ of a system with dynamic backlash for $\omega = \{15, 20, 25, 35, 40\}$ rad/s and $\varepsilon = \{0.2, 0.5, 0.8\}$. The charts reveal that we can have chaotic or periodic responses according with the values of ω and ε.

A complementary perspective is revealed by Figure 15 that depicts the number of consecutive collisions on side A (or B), n_A (or n_B), *versus* the exciting frequency ω and the coefficient of restitution ε for an input force $f(t) = 50\cos(\omega t)$.

From Figure 15 we can distinguish two kinds of regions. The first, for $\omega_C < \omega < \omega_J$, where the system is characterized by an irregular number of impacts and a chaotic dynamics. The second, for $\omega_J < \omega < \omega_L$, where the motion is characterized by a regular behaviour corresponding to one alternate collision on each side of M_1. The conclusions are similar to those obtained from Figures 10–14.

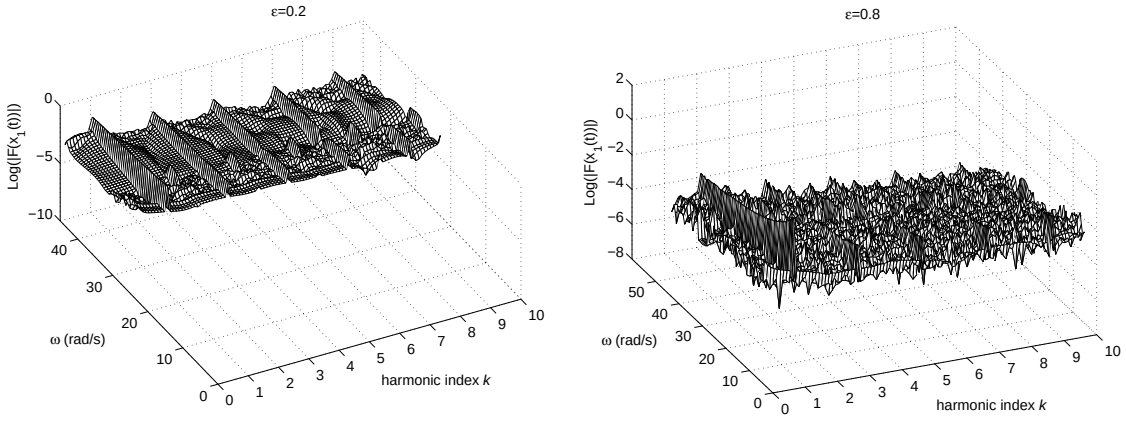

Figure 9: Fourier transform of the output displacement $x_1(t)$, $F\{x_1(t)\}$, over 20 cycles, *versus* the exciting frequency ω and the harmonic index k, for $\varepsilon = \{0.2, 0.8\}$

Model not applicable. For ε = 0.2 it results a lower-limit frequency ω_C = 23.9 rad/s.

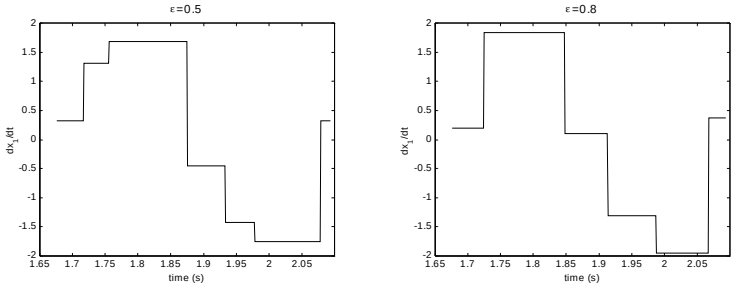

Figure 10: Plot of the output velocity $\dot{x}_1(t)$ for ω = 15 rad/s and ε = {0.2, 0.5, 0.8}

Model not applicable. For ε = 0.2 it results a lower-limit frequency ω_C = 23.9 rad/s.

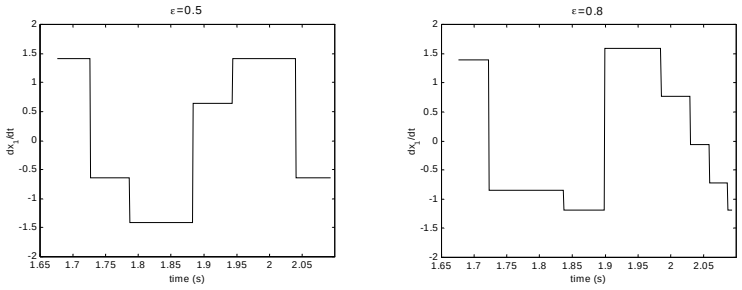

Figure 11: Plot of the output velocity $\dot{x}_1(t)$ for ω = 20 rad/s and ε = {0.2, 0.5, 0.8}

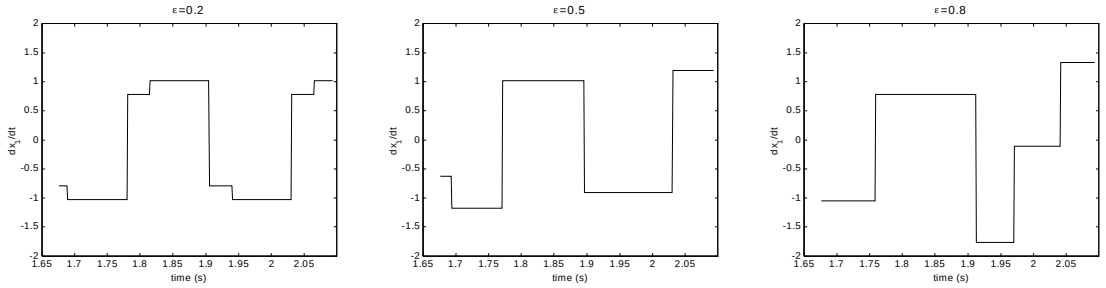

Figure 12: Plot of the output velocity $\dot{x}_1(t)$ for ω = 25 rad/s and ε = {0.2, 0.5, 0.8}

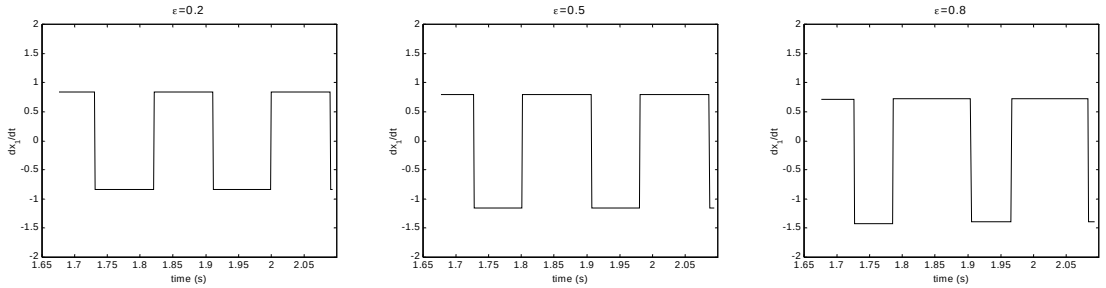

Figure 13: Plot of the output velocity $\dot{x}_1(t)$ for ω = 35 rad/s and ε = {0.2, 0.5, 0.8}

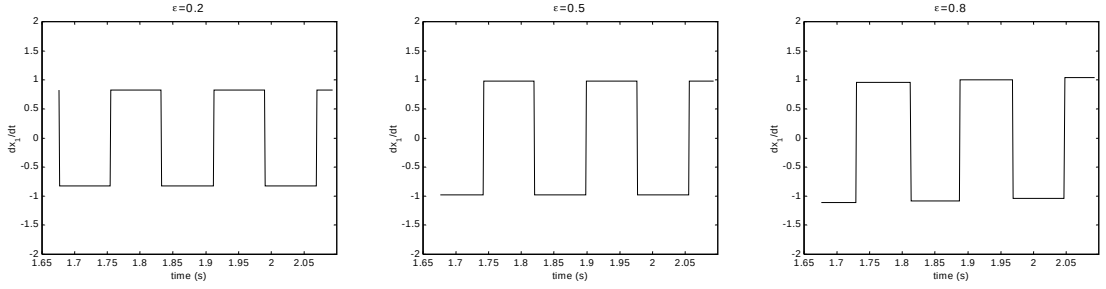

Figure 14: Plot of the output velocity $\dot{x}_1(t)$ for ω = 40 rad/s and ε = {0.2, 0.5, 0.8}

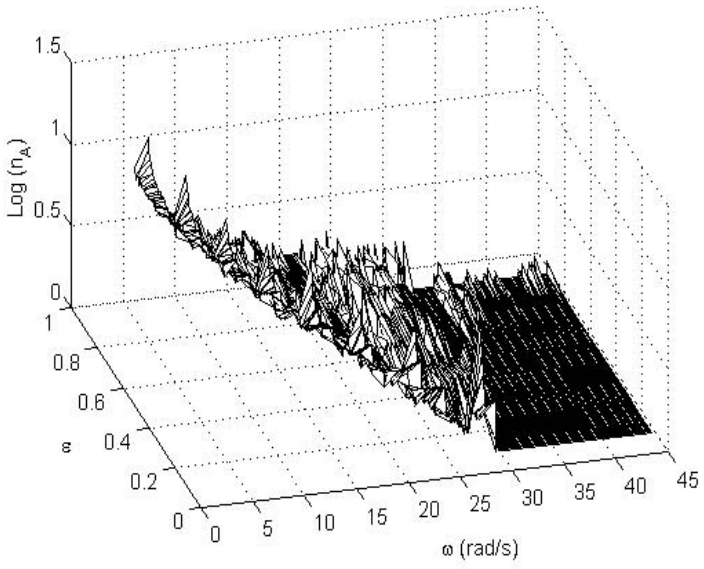

Figure 15: Number of consecutive collisions on side A (n_A) *versus* the exciting frequency ω and the coefficient of restitution ε, for an input force $f(t) = 50\cos(\omega t)$. For the side B (n_B) the chart is of the same type

4 Conclusions

This paper addressed several aspects of the phenomena involved in systems with backlash and impacts. The dynamics of a two mass system was analysed through the describing function method and compared with standard models. The results revealed that these systems might lead to chaos and to fractional order dynamics. These conclusions encourage further studies of nonlinear systems in the perspective of the fractional calculus since integer order dynamical models are not capable to take into account many phenomena that occur.

References

[1] K. B. Oldham and J. Spanier. *The Fractional Calculus*. Academic Press, New York, 1974.

[2] S. G. Samko, A. A. Kilbas and O. I. Marichev. *Fractional Integrals and Derivatives*. Gordon and Breach Science Publishers, Amsterdam, 1993.

[3] K. S. Miller and B. Ross. *An Introduction to the Fractional Calculus and Fractional Differential Equations*. John Wiley & Sons, New York, 1993.

[4] I. Podlubny. *Fractional Differential Equations*. Academic Press, San Diego, 1999.

[5] R. Hilfer. *Applications of Fractional Calculus in Physics*. World Scientific, Singapore, 2000.

[6] A. Gemant. A Method of Analyzing Experimental Results Obtained from Elasto-Viscous Bodies. *Physics*, 7: 311–317, 1936.

[7] R. L. Bagley and P. J. Torvik. Fractional Calculus-A Different Approach to the Analysis of Viscoelastically Damped Structures. *AIAA Journal*, 21(5): 741–748, 1983.

[8] L. Rogers. Operators and Fractional Derivatves for Viscoelastic Constitutive Equations. *Journal of Rheology*, 27(4): 351–372, 1983.

[9] R. C. Koeller. Applications of Fractional Calculus to the Theory of Viscoelasticity. *ASME Journal of Applied Mechanics*, 51: 299–307, 1984.

[10] N. Makris and M. C. Constantinou. Fractional-Derivative Maxwell Model for Viscous Dampers. *Journal of Structural Engineering*, 117(9): 2708–2724, 1991.

[11] L. Gaul and M. Schanz. Dynamics of Viscoelastic Solids Treated by Boundary Element Approaches in Time Domain. *European Journal of Mechanics*, *A/Solids*, 13(4) – suppl.: 43–59, 1994.

[12] Åsa Fenander. Modal Synthesis when Modeling Damping by Use of Fractional Derivatives. *AIAA Journal*, 34(5): 1051–1058, 1996.

[13] T. T. Hartley, C. F. Lorenzo and H. K. Qammer. Chaos in Fractional Order Chua's System. *IEEE Transactions on Circuits and Systems-I: Fundamental Theory and Applications*, 42(8): 485–490, 1995.

[14] B. Mandelbrot. *The Fractal Geometry of Nature*. W. H. Freeman and Company, New York, 1983.

[15] A. Méhauté. *Fractal Geometries: Theory and Applications*. Penton Press, London, 1991.

[16] Fernando B. Duarte and J. A. Tenreiro Machado. Chaotic Phenomena and Fractional-Order Dynamics in the Trajectory Control of Redundant Manipulators. *Nonlinear Dynamics,* 29(1–4): 315–342, July 2002.

[17] T. J. Anastasio. The Fractional-Order Dynamics of Brainstem Vestibulo-oculomotor Neurons. *Biological Cybernetics*, 72: 69–79, 1994.

[18] H. M. Ozaktas, Z. Zalevsky and M. A. Kutay. *The Fractional Fourier Transform*. John Wiley & Sons, Chichester, 2001.

[19] B. Mathieu, L. Le Lay and A. Oustaloup. Identification of Non Integer Order Systems in the Time Domain. In *Proceedings of the IEEE SMC/IMACS Symposium on Control, Optimization and Supervision*, pages 952–956, Lille, France, 1996.

[20] F. Mainardi. Fractional Relaxation-Oscillation and Fractional Diffusion-Wave Phenomena. *Chaos, Solitons & Fractals*, 7(9): 1461–1477, 1996.

[21] R. Gorenflo and F. Mainardi. Random Walk Models for Space-Fractional Diffusion Processes. *FCAA Fractional Calculus and Applied Analysis*, 1(2): 167–191, 1998.

[22] N. Engheta. On the Role of Fractional Calculus in Electromagnetic Theory. *IEEE Antennas and Propagation Magazine*, 39(4): 35–46, 1997.

[23] A. Méhauté. From Dissipative and to Non-dissipative Processes in Fractal Geometry: The Janals. *New Journal of Chemistry*, 14(3): 207–215, 1990.

[24] A. Oustaloup. *La Commande CRONE: Commande Robuste d'Ordre Non Entier*. Hermes, Paris, 1991.

[25] J. A. Tenreiro Machado. Analysis and Design of Fractional-Order Digital Control Systems. *SAMS Journal Systems Analysis, Modelling, Simulation*, 27: 107–122, 1997.

[26] J. A. Tenreiro Machado. Discrete-Time Fractional-Order Controllers. *FCAA Fractional Calculus and Applied Analysis*, 4(1): 47–66, 2001.